Glaciochemical reconnaissance of a new ice core from Severnaya Zemlya, Eurasian Arctic

Karin WEILER,[1*] Hubertus FISCHER,[1] Diedrich FRITZSCHE,[2] Urs RUTH,[1,3] Frank WILHELMS,[1] Heinz MILLER[1]

[1]*Alfred Wegener Institute for Polar and Marine Research, PO Box 120161, D-27515 Bremerhaven, Germany*
E-mail: weiler@climate.unibe.ch
[2]*Alfred Wegener Institute for Polar and Marine Research, PO Box 600149, D-14473 Potsdam, Germany*
[3]*Institute for Environmental Physics, University of Heidelberg, Im Neuenheimer Feld 299, D-69120 Heidelberg, Germany*

ABSTRACT. A deep ice core has been drilled on Akademii Nauk ice cap, Severnaya Zemlya, Eurasian Arctic. High-resolution chemical analysis has been carried out for the upper 53 m of this ice core to study its potential as an atmospheric aerosol archive, despite strong meltwater percolation. These records show that a seasonal atmospheric signal cannot be deduced. However, strong year-to-year variations have allowed the core to be dated, and a mean annual net mass balance of 0.46 m w.e. a^{-1} was deduced. The chemical signature of an extraordinarily high peak in electrical conductivity at 26 m depth pointed clearly to the eruption of Bezymianny, Kamchatka, in 1956. However, in general, peaks in the electrical conductivity are not necessarily related to deposition of volcanogenic sulphur aerosol. In contrast, maximum sulphate and nitrate concentrations in the ice could be related to maximum SO_2 and NO_x anthropogenic emissions in the 1970s, probably caused by the nickel- and copper-producing industries in Norilsk and on the Kola peninsula or by industrial combustion processes occurring in the Siberian Arctic. In addition, during recent decades sulphate and nitrate concentrations declined by 80% and 60%, respectively, reflecting a decrease in anthropogenic pollution of the Arctic basin.

1. INTRODUCTION

Ice-core archives provide unique information about the physical and chemical properties of the atmosphere in the past. Most of the investigations leading to high-resolution chemical records for the Northern Hemisphere were performed in the dry snow zone (e.g. in Greenland) while information from other Arctic glaciers outside the dry snow zone, like Severnaya Zemlya, is sparse and often complicated by meltwater percolation.

Between 1978 and 1988, eight ice cores were drilled on the archipelago Severnaya Zemlya (Kotlyakov and others, 2004), in the easternmost part of the Eurasian Arctic (see Fig. 1). Chemical analysis of these ice cores was restricted to a few components only, with emphasis on Cl^- (Arkhipov, 1999; Kotlyakov and others, 2004), as published, for instance, by Vaikmyae and Punning (1982) for a 556 m deep ice core from Vavilov ice cap (79° N, 96° E) drilled in 1978. The Cl^- record presented by these authors covers the top 400 m, but sample resolution was relatively coarse except for three small intervals where the Cl^- profile is given in 2 cm steps. Additional chemical components were measured on the only ice core that had previously been drilled to bedrock (761 m) on Akademii Nauk ice cap in 1986/87 (80.50° N, 94.83° E). Concentration values for SO_4^{2-}, Cl^-, Na^+, Mg^{2+}, Ca^{2+} and K^+ down to 562 m depth for this ice core, as well as a summary of data obtained from other Arctic ice cores, are provided at http://www.pangea.de/PangaVista?query=ddga (Arkhipov, 1999). Data resolution is often quite coarse, however. For the Akademii Nauk ice core, for example, resolution ranges from 2 to 10 m of core and decreases with depth.

In this paper, we present the first high-resolution (on average 60 mm sample length) chemical ice-core records from Severnaya Zemlya, derived from analyses of the uppermost 53 m of a 723.9 m long ice core drilled during the 1999–2001 field seasons on Akademii Nauk ice cap (80°31′ N, 94°49′ E; 760 m a.s.l.) (Fritzsche and others, 2002), marked on Figure 1. With an ice thickness of 723.9 m and a mean annual temperature of approximately –18°C, this ice cap is the thickest and coldest in Severnaya Zemlya. The mean annual temperature has been deduced from the mean annual temperature, –14.7°C, of the nearby weather station, Golomyanny (available at http://npolar.no/transeff/transport/ice/AARI_chapter3riktig.pdf (Alexandrov and others, 2000)), corrected by the temperature gradient relative to weather-station data from Akademii Nauk (Kuhn, 2000) obtained in 1999 (Fritzsche, unpublished information).

As it is located in the easternmost part of the Eurasian Arctic, different atmospheric information can be expected from this ice-core archive than that obtained from the Greenland and other Arctic ice caps. From trajectory analysis (850 hPa level in March/April; Vinogradova and Egorov, 1996) it is determined that Severnaya Zemlya is mainly influenced by air masses originating over Europe, northern Eurasia and the Atlantic Ocean, whereas a large part of the air masses (back trajectories on the 700 hPa level; Kahl and others, 1997) reaching Summit, Greenland, pass the Canadian Arctic and enter Greenland from the west throughout the year.

Furthermore, from investigations carried out on Greenland it has been observed that episodes of increased aerosol input (e.g. due to Arctic haze events (Shaw, 1995)) are reflected at Dye 3 (2479 m a.s.l.) with lower concentrations and for shorter durations compared to sea-level sites (Davidson and others, 1993). Thus, it is expected that Arctic

*Present address: Climate and Environmental Physics, Physics Institute, University of Bern, Sidlerstrasse 5, CH-3012 Bern, Switzerland.

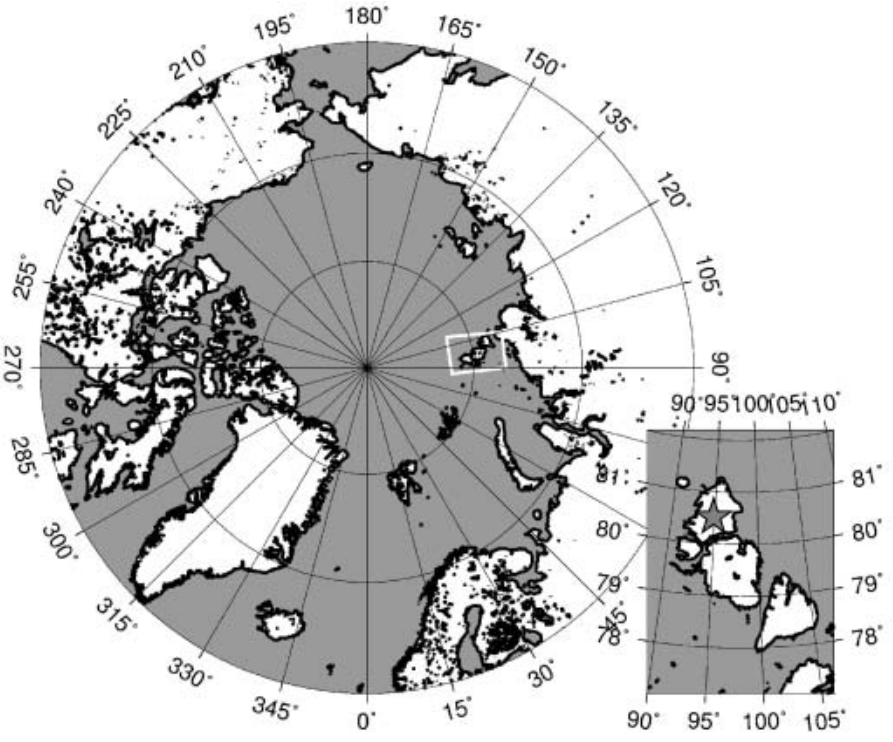

Fig. 1. Map of the Arctic. The ice core was drilled on Akademii Nauk ice cap (80°31′ N 94°49′ E, star) the northernmost island of Severnaya Zemlya.

haze events especially will be more pronounced at Severnaya Zemlya due to the lower altitude of this ice cap. Accordingly, Severnaya Zemlya represents an ideal location to monitor atmospheric circulation in the Siberian Arctic and to reconstruct the history of anthropogenic air pollution in this area. However, summer temperatures can exceed 0°C at this drill site, as was the case for a few days in August 1999, seen in automatic weather station data (Kuhn, 2000). Maximum monthly mean air temperatures for 1999 were found for July (–1.1°C) and August (–1.4°C). Slight surface melting was observed at the end of May 1999 (Fritzsche, unpublished information). These melting processes lead to downward percolation of meltwater and thus to a redistribution of the physical and chemical core parameters. One purpose of this study is to estimate the extent to which parameters detectable in the ice are influenced by summer melting.

The interpretation and discussion of the data are focused on the following aspects:

On what time-scale can undisturbed atmospheric information be deduced? Do variations in the chemical records reflect seasonal cycles or are they a result of the melting processes? This aspect is closely related to the dating of the ice. A method for deriving a depth-to-age relationship for this ice core will be presented.

Are maxima in the electrical conductivity record linked to volcanic events, as is the case in the dry snow zone (Herron, 1982)?

What is the long-term anthropogenic influence on the SO_4^{2-} and NO_3^- content in an ice core due to strong summer percolation?

2. METHODS OF SAMPLE PREPARATION AND CHEMICAL ANALYSIS

At the Alfred Wegener Institute (AWI), Bremerhaven, Germany, high-resolution measurements of electrical conductivity (dielectric profiling: Wilhelms and others, 1998; Wilhelms, 2000) and density (γ-absorption method: Wilhelms, 2000) were carried out. The stratigraphy of the ice was recorded using a line-scanning camera (Wilhelms and others, 1997).

A total of 450 ice samples were prepared for chemical analysis. To this end, rectangular ice strips with a cross-section of 30 mm × 40 mm and a length of about 500 mm were cut from the inner part of the ice core. To decontaminate the ice, a ~2 mm thick layer was removed from the whole surface under a clean bench using a contamination-free electromechanical plane (Fischer and others, 1998a). Aliquots with a mean depth resolution of 60 mm (corresponding to 8–9 samples per year) were then prepared using a contamination-free circular saw, and sealed in pre-cleaned polyethylene (PE) bags for storing in a cold room to await measurement.

Melted decontaminated ice samples were analyzed for anions (methanesulphonate (MSA^-), Cl^-, NO_3^-, SO_4^{2-}) and cations (Na^+, NH_4^+, Mg^{2+}, Ca^{2+}) using a Dionex IC20 ion chromatograph. Blank samples were measured routinely by processing ultrapure water ice (Milli-Q water; specific resistance >18.2 MΩ cm) together with the core samples.

The PE bags and tools needed for further work were precleaned by rinsing them with ultrapure water until the remnant conductivity of the water was $<0.8\,\mu S\,cm^{-1}$ for the PE bags and the PE vials for the ion chromatograph, $<0.5\,\mu S\,cm^{-1}$ for the PE bottles in which the melted aliquots were stored, and $<1\,\mu S\,cm^{-1}$ for the tools needed to handle the samples in the clean laboratory.

Table 1. Summary of the concentration limits and concentration errors derived for the various ions. The numbers of samples with a concentration error larger then 10% are listed. Values in parentheses correspond to around 50% of the samples which have been measured at a different time and with a slightly different system

Ion species	Concentration limit (derived from blank values)		Concentration error		Number of samples from 435 (495) with concentration error >10%
	Lower limit ng g^{-1}	Upper limit ng g^{-1}	Lower limit %	Upper limit %	
Na^+	1 (10)	1000	26.7 (17.0)	0.7 (2.1)	0 (2)
Cl^-	5 (5)	2500	11.8 (11.7)	1.2 (0.9)	0 (1)
SO_4^{2-}	5 (12.5)	2500	9.5 (7.8)	1.4 (1.3)	0 (0)
MSA^-	1 (2.5)	500	20.4 (11.7)	12 (3.1)	45 (38)
Ca^{2+}	3 (5)	500	23.6 (6.1)	1 (5.3)	134 (0)
Mg^{2+}	1 (2.5)	500	25.6 (9.1)	1.1 (5.6)	10 (0)
NO_3^-	5 (12.5)	2500	24.3 (10.4)	0.6 (4.7)	2 (0)
NH_4^+	3 (25)	500	28.1 (11.3)	1.3 (2.0)	41 (29)

In Table 1 the lower concentration limits (which are derived from comparison of the blank-samples concentrations with the response function of the system) and the upper concentration limits (defined by external calibration standards) are summarized for the different ions. The corresponding concentration errors (lower and upper limit) are also listed. The values in parentheses correspond to around half of the samples, which have been measured at a different time and with a modified system. Note that the error decreases with increasing ion concentration due to the decreasing impact of the blank sample values. The number of samples with a concentration error >10% shows that the majority of the detected ion concentrations are well above the lower concentration limit except for Ca^{2+}, NH_4^+ and MSA^-. The discrepancy is caused by a slight contamination of the Ca^{2+} samples during the preparation process in the laboratory and an intensive variation in laboratory background concentrations for NH_4^+. In the case of MSA^-, a poorer baseline definition of the system is the reason.

3. RESULTS AND DISCUSSION

3.1. The reflection of atmospheric seasonality in the ion records

The concentration of various chemical components which are distributed in the Arctic atmosphere varies during the year due to a change in the meteorological circulation pattern, mainly associated with the seasonal migration of the polar front (Rahn and others, 1977). Consequently, a seasonal oscillation in the ion records of ice cores drilled in the dry snow zone (e.g. in central Greenland) can be interpreted as a seasonal variation in atmospheric concentration and then used to distinguish individual years (Steffensen, 1988; Beer and others, 1991; Fischer and others, 1998a). At Akademii Nauk ice cap, however, melting and refreezing processes occur and the snowpack stratigraphy is disturbed. Further, ion fractionation processes may be expected, owing to differences in elution strength of individual ion species.

Snow lysimeter experiments carried out by Johannessen and Henriksen (1978) show that the first 30% of water to melt contains 44–76% of the total amount of all examined chemical components (including sea salt, mineral dust, sulphate and nitrogen components). Furthermore, SO_4^{2-} and NO_3^- are eluted from snow more rapidly than, for instance, Cl^- or Na^+ (Goto-Azuma and others, 1993, 1995). Investigations by Davies and others (1982) show a stronger mobility within the snow for Cl^- than for Na^+. Additionally, the degree of elution depends on the duration of different melt/freeze cycles, the melting rate and the initial distribution of the impurities in the snowpack as well as the location of the ions in the crystal lattice or on the surface of the ice grains (Mulvaney and others, 1988; Davis and others, 1995).

At Akademii Nauk, the influence of the melting processes on the behaviour of the ion signal, the conductivity and the density of the ice can be deduced from the visual ice-core stratigraphy (Fig. 2). As expected for ice drilled in the percolation snow zone (Benson, 1961), the occurrence of periodic melting events often leads to the penetration of pure firn by vertical pipe-like percolation channels (darker sectors with lower density) and ice lenses and layers (white strata; density near 0.91 g cm^{-3}) (Schütt and others, 2003). Furthermore, these ice layers seem to correlate with high signals in electrical conductivity, where maximum values can often be found in or at the edge of an ice layer. As the conductivities of the different ions are reflected in the electrical conductivity of the ice, this supports the assumption that the ion profile is strongly affected by melting.

For that reason, it is not possible to link the ionic ice-core records to the seasonal cycles of the chemical composition of the atmosphere. However, the ion profile can be considered as an annually varying melting/refreezing signal, from which a counted depth-to-age relation can be deduced.

3.2. Dating the ice core by counting sodium cycles

The chemical profile and the stratigraphic record of the ice core show periodic features as illustrated in Figure 2. Assuming the annual snow accumulation is affected by melting processes in a similar manner each year, it is possible to use these cycles to mark individual years. Thus, it can be assumed that ice layers formed from firn penetrated by meltwater operate as barriers for further penetration (Goto-Azuma and others, 1993; Schütt and others, 2003) and therefore lead to an accumulation of chemical components above them (see, e.g., the Na^+ peak between 2.6 and 2.8 m in Fig. 2). From counting these ion peaks, the number of years in a certain depth range can be obtained.

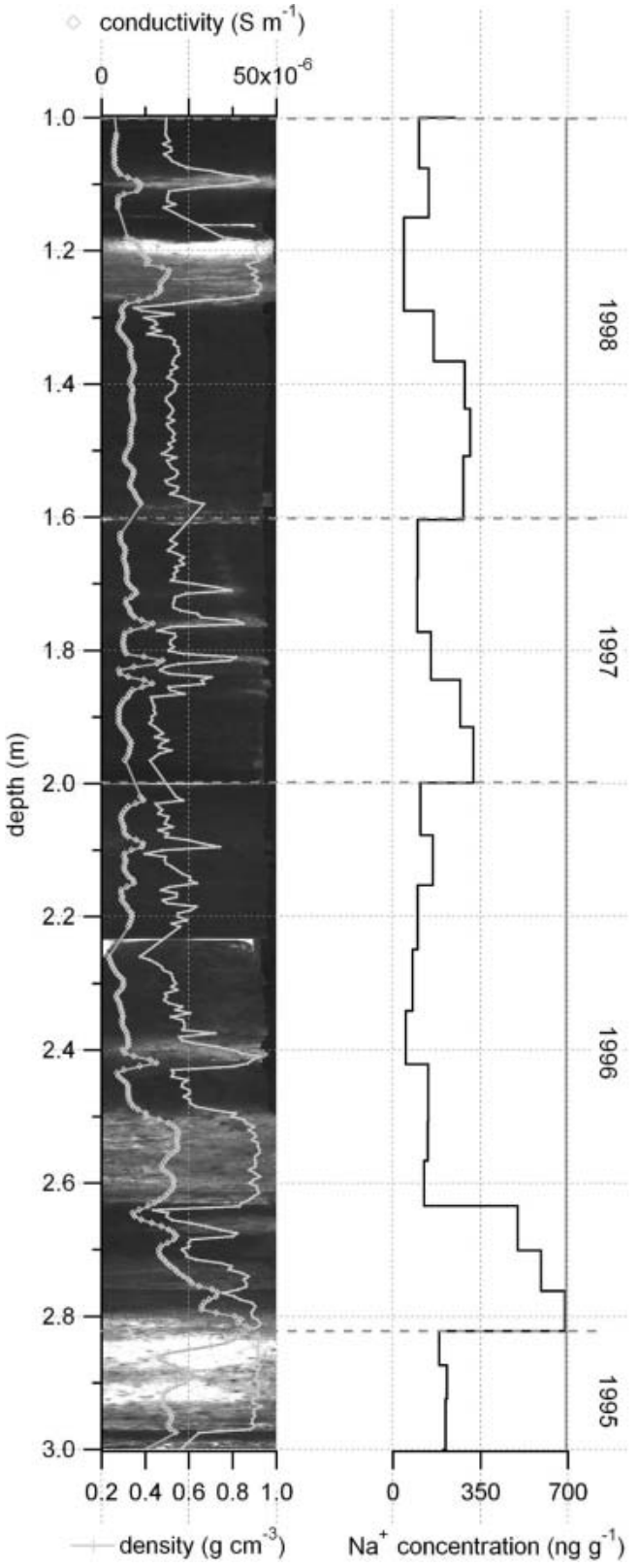

Fig. 2. Visual ice-core stratigraphy plotted against the core depth in metres. The electrical conductivity (grey diamonds) and the ice density (grey line) are shown, as well as the Na^+ record (black line). Single years as deduced from counting Na^+ cycles are marked by dashed grey horizontal lines.

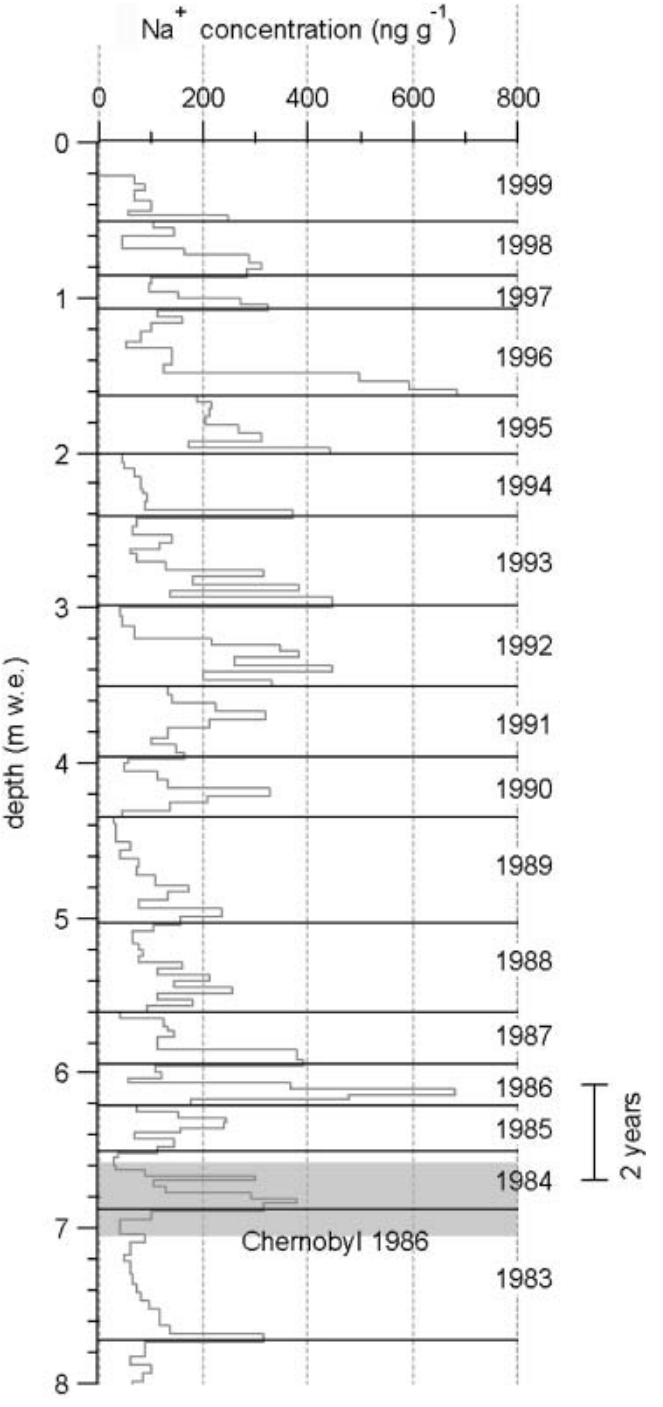

Fig. 3. Na^+ profile plotted against core depth in m w.e. (grey line). Black lines indicate the boundaries between different years. Note that no seasonal atmospheric information can be deduced with this method. The Chernobyl horizon (derived from the ^{137}Cs record) is depicted as a grey rectangle.

As an example, in Figure 3 the top few metres of the Na^+ concentration profile are plotted against the core depth. Black lines are used to indicate the boundaries between different years according to the recurring pattern in the Na^+ record. The Na^+ record was chosen, firstly, because the mean Cl^- to Na^+ ratio (2.00 ± 0.63) is close to that of sea water (1.84). This indicates that essentially all of the Na^+ detected at Severnaya Zemlya is of sea-salt origin. Thus, compared to the other chemical components, the signal is influenced by one source only and no anthropogenic contribution needs to be considered. Secondly, Na^+ has a lower mobility than NO_3^- and SO_4^{2-}, and is therefore least affected by elution processes (see section 3.1).

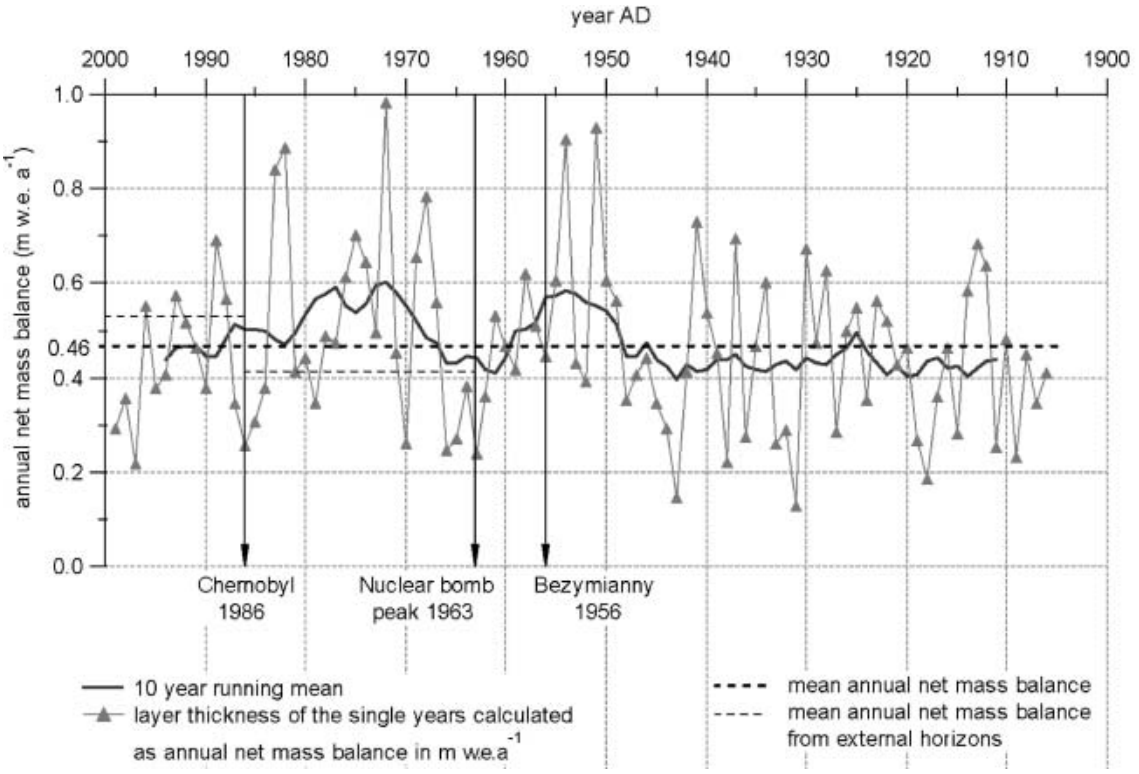

Fig. 4. Annual layer thickness derived from counting Na^+ cycles (grey triangles). The annual net accumulation as derived from a 10 year running mean is indicated by a black line. The mean annual net mass balance is shown as a thick dashed black line. The mean annual net mass balances deduced from the external reference horizons are depicted as thin dashed black lines. Note that the Chernobyl horizon was detected on a shallow ice core drilled close to the main core.

To confirm this approach, external reference horizons have been considered. A maximum of the ^{137}Cs activity at 21.36–22.68 m depth was identified as the 1963 layer corresponding to fallout from the atmospheric nuclear bomb tests in 1961–62 (Pinglot and others, 2003). In addition, on the shallow core SZ 2000-1, a second ^{137}Cs peak was identified at 10.19–10.89 m depth (converted to the 1999 surface using the mean annual net mass balance derived from SZ 2000-1), reflecting the Chernobyl accident in 1986 (for details see Fritzsche and others, 2002).

The age obtained by counting Na^+ cycles agrees, within 2 years, with the Chernobyl horizon in 1986 (Fig. 3, grey shaded area), which itself may be shifted to deeper layers by meltwater percolation (Pinglot and others, 2003). Furthermore, it has to be considered that, especially due to the summer melting, strong horizontal variations in the surface structure of the firn are likely (snow-pit studies; Ruth, unpublished information). Therefore, an error in the depth assignment of this reference layer, caused by the matching of the shallow core with the main core, cannot be excluded.

Following this procedure, an age discrepancy of 4 years is observed for the nuclear-bomb peak in 1963. A discrepancy of 3 years is found for a strong peak in the electrical conductivity record at 25.86 m depth. This peak is assumed to be the result of the eruption of the Bezymianny (Kamchatka) volcano in 1956 (see also section 3.4). For these two horizons it has to be considered that the percentage of firn ice is <30%, sometimes <10%, for this depth range (personal communication from R. Schütt). Thus, it is likely that the accumulation for some years, and therefore the corresponding Na^+ cycles, are missing completely.

The good agreement between the number of Na^+ cycles and the various reference horizons indicates the method is useful for dating this ice core. For the whole depth range, 94 years could be counted, placing 1906 at 53 m depth, with a maximum dating error of –4 to +2 years to 26 m depth and probably with a larger error below this depth, where no more reference horizons are available.

A similar approach has been used to date various other ice cores subjected to summer melting: for instance, the top 42.5 m of a 84 m deep ice core from Snøfjellafonna, Svalbard (Goto-Azuma and others, 1995), where Na^+ cycles were counted with a dating accuracy of ± 2 or ± 3 years above the 1963 bomb peak horizon, and possibly less accuracy below this depth, since no additional reference horizons could be documented in the deeper part of this core. Counting of seasonal cycles in the chemical profiles was also used to date a 122 m ice core from Lomonosovfonna, Svalbard (Kekonen and others, 2002), where, in addition to the 1963 radioactive layer, the Laki (Iceland) eruption could be detected as a supplementary reference.

3.3. Mean net accumulation for the 20th century

As shown above, a continuous depth-to-age relationship can be established by counting annual Na^+ melt cycles. With this result, it is possible to determine the thickness of each annual layer (Fig. 4, grey triangles). However, annual layer thickness is not necessarily equal to the snow accumulation for the corresponding years, since meltwater transport in and out of these layers has occurred. Therefore, the annual mean net accumulation is estimated as a mean value for a core section for which the loss of mass compared to the total

Table 2. Total peak load and total peak load ratio calculated for $nssSO_4^{2-}$ and $nssCl^-$ for three extraordinarily high maxima in the electrical conductivity record at depths of approximately 20, 26 and 44 m. As a background value, the mean total peak load ratio, which was computed from the average of the total peak load ratios contributed by peaks above and below the corresponding maximum in the electrical conductivity record, is listed (for details see text)

Ion species	Total peak load single ions*			Total peak load ratio†			Mean total peak load ratio (background)		
	20 m	26 m	44 m	20 m	26 m	44 m	20 m	26 m	44 m
	10^3 μeq m^{-2}	10^3 μeq m^{-2}	10^3 μeq m^{-2}	%	%	%	%	%	%
$nssSO_4^{2-}$	8.4	28.7	9.4	31.5	28.6	12.5	25.0	12.4	6.9
$nssCl^-$	–1.4	11.2	0.5	–5.2	11.1	0.6	1.4	3.9	2.0

*$\sum_j [Ion]_i \cdot \Delta z_{j,\mathrm{m\,w.e.}}$.

†Total peak load ratio $= \dfrac{\sum_j [Ion]_i \cdot \Delta z_{j,\mathrm{m\,w.e.}}}{\sum_i \left(\sum_j [Ion]_i \cdot \Delta z_{j,\mathrm{m\,w.e.}} \right)} \times 100\%$.

i: indicator for different ion species $[Ion]_i$ in μeq kg^{-1}.
j: counting depth steps $\Delta z_{\mathrm{m\,w.e.}}$.

snow amount can be assumed to be negligible (approximately 10 years).

A mean net accumulation of 0.46 m w.e. a^{-1} (Fig. 4, dashed thick black line) is deduced for Akademii Nauk from a 10 year running mean (black line, Fig. 4) covering approximately the last 100 years BP. This value fits well with the observations of Zagorodnov and others (1990), who deduced a mean annual net mass balance of 0.43–0.44 m w.e. a^{-1} from structural stratigraphic methods. Other results for the accumulation at Akademii Nauk ranging from 0.23 to 0.29 m w.e. a^{-1}, as summarized by Kotlyakov and others (2004), could not be confirmed.

Note that variations in the temporal evolution of the net accumulation between around 1950 and 1980 mainly reflect the dating error and thus do not represent the natural variation in precipitation. As mentioned above, the definition of individual years in the record, as well as the transfer of the Chernobyl horizon from the shallow core to the main core, may also affect the dating error. This is why the mean annual net mass balances independently calculated from the external reference horizons (Fig. 4, thin dashed lines) differ from the values achieved from averaging the layer thicknesses.

3.4. Specific events

Major volcanic eruptions release large quantities of impurities into the atmosphere which often lead to significantly higher concentrations of non-sea-salt (nss) SO_4^{2-} and, in some instances, also $nssCl^-$. Thus, maxima in the electrical conductivity of the ice onto which these impurities are deposited are recorded (Herron, 1982). The non-sea-salt portion of an ion species is calculated as the difference between the total concentration and the sea-water contribution as represented by the Na^+ concentration.

In the Academii Nauk ice core, three extraordinarily high conductivity peaks at depths of around 20, 26 and 44 m (black diamonds; see Fig. 5a–c), which were initially suspected to be of volcanic origin, were analyzed for their chemical composition. As can be seen from Figure 5, higher ion concentrations are detectable not only for volcanogenic components but for all ion species in these peaks. Thus maxima in electrical conductivity cannot be linked directly to volcanic eruptions, as is normally assumed for ice cores drilled in the dry snow zone. Instead, these peaks seem to be the result of ion fractionation processes caused by melting/refreezing cycles (see section 3.1). This assumption is also supported by the locations of the ion maxima within ice layers (20 and 44 m depth) or between two ice layers (26 m depth; see Fig. 5).

Similar observations have been made using other cores affected by summer melting. In the case of the core from Snøfjellafonna, Spitsbergen (Goto-Azuma and others, 1995), no clear volcanic signal could be detected, as extremely high concentrations of SO_4^{2-} (4178.8 ng g^{-1}) dated to around 1940 were accompanied by strong maxima in Na^+, Cl^- and NO_3^-. The same pattern occurred in an ice core from Penny Ice Cap, Baffin Island, Canada (Grumet and others, 1998), where evidence for a considerable peak in the $nssSO_4^{2-}$ (around 1914, almost 800 ng g^{-1}) associated with the eruption of Katla, Iceland (1918), could only be substantiated by the presence of basaltic glass, as the dust-related species showed high concentration values, too.

In the case of Akademii Nauk, the conductivity maximum detected at 26 m depth can be attributed to the eruption of Bezymianny in 1956 (volcanic explosivity index (VEI) = 5; Simkin and Siebert, 1994). This is done by comparison of the total peak load ratio for the event relative to the background. The total peak load ratio compares the peak area (peak load), calculated for a specific ion $[Ion]_i$ with the total peak load (sum of the peak loads contributed by every single ion species; for definitions see footnotes in Table 2). This measure is independent of peak width or height. As a background value, the mean total peak load ratio will be considered. This is the average of the total peak load ratios contributed by three or four smaller peaks located directly above or below the corresponding conductivity peak. The three or four smaller peaks are chosen to be representative of the contemporary conditions in atmospheric concentrations and meltwater percolation in the snowpack.

As can be seen from Table 2, the percentage of $nssSO_4^{2-}$ in the total peak load ratio at 26 m (28.6%) is more than twice the corresponding background value (12.3%). Much smaller contributions are observed for the 20 and 44 m maxima. Additionally, a $nssCl^-$ contribution of 11.1% is observed for the conductivity maximum at 26 m. This value is exceptionally high compared to the corresponding

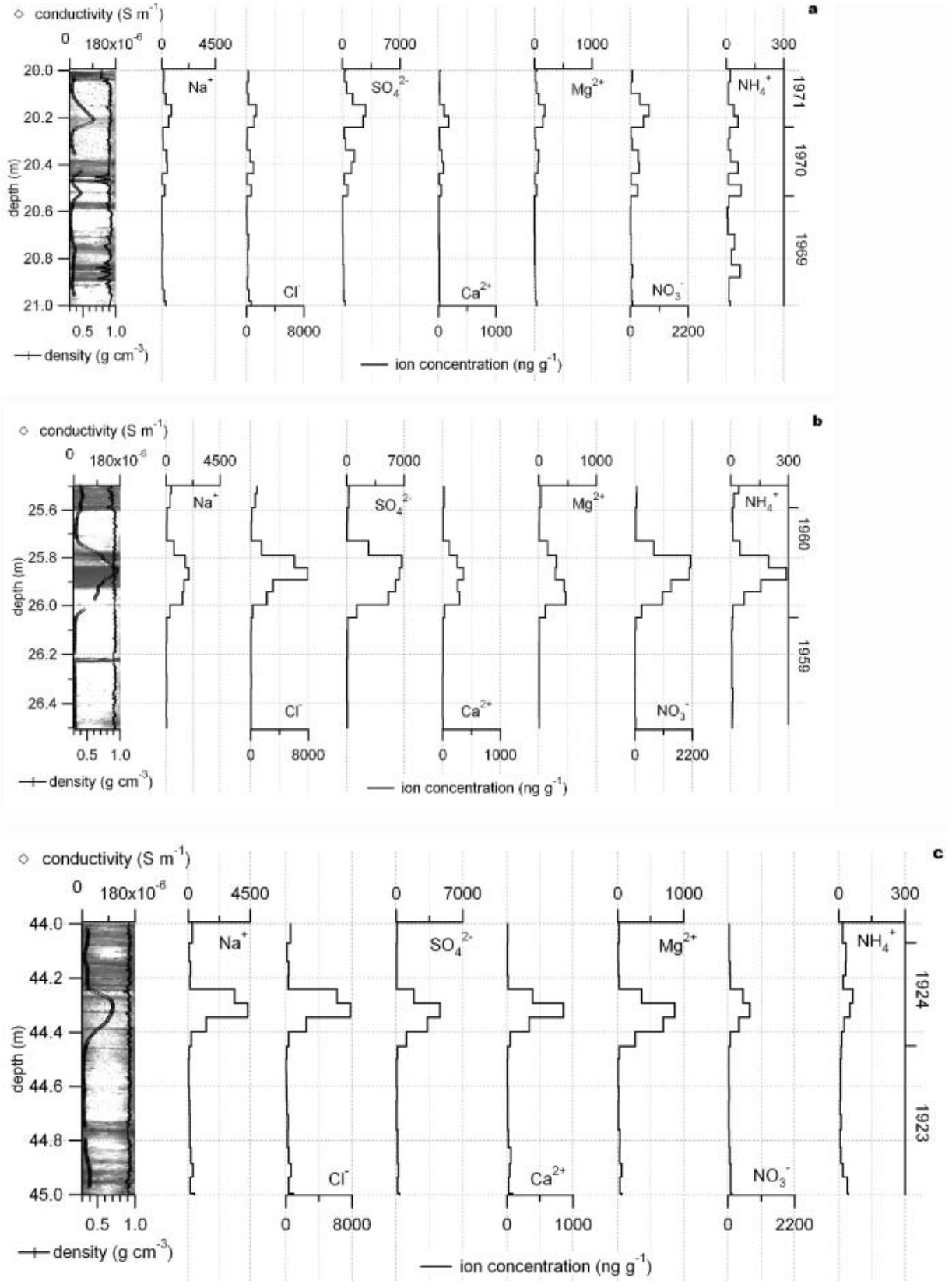

Fig. 5. Ion profiles for three extraordinarily high peaks in the electrical conductivity record (black diamonds) at around (a) 20 m, (b) 26 m and (c) 44 m depth. Concentrations of the different ions (black lines), corresponding core stratigraphy and the density signal (black line) are shown on the left.

mean total peak load ratio of 3.9%. In the case of the maximum at 44 m depth, the total nssCl^- peak load ratio is much lower compared to the background value, and for the 20 m horizon a negative nssCl^- contribution is found. Accordingly, the relative contribution of nssSO_4^{2-} and nssCl^- to the total peak load at 26 m is higher than expected from background conditions, supporting a volcanic origin of this horizon.

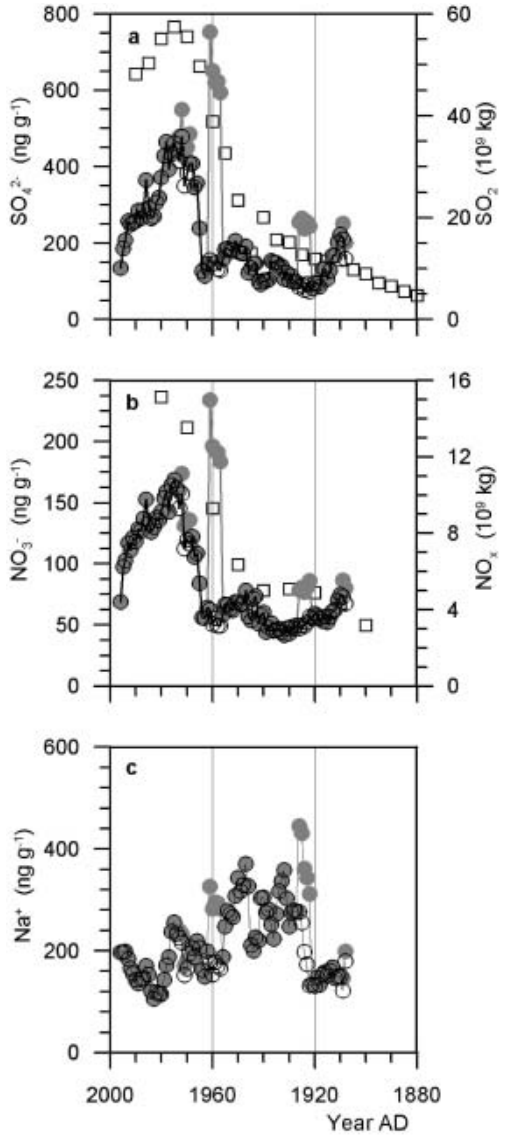

Fig. 6. Long-term variations in the (a) nssSO_4^{2-}, (b) nssNO_3^- and (c) nssNa^+ concentrations detected at Akademii Nauk derived from water-weighted 5 year running averages. The grey circles represent the raw data; open circles depict the result after removing samples suspected to be influenced by volcanic input (around five samples for each horizon at approximately 20, 26 and 44 m; see Fig. 4). Open squares indicate total (a) Eurasian SO_2 (Mylona, 1996) and (b) European NO_x emissions (Hov and others, 1987).

According to Simkin and Siebert (1994), no strong volcanic events (with VEI > 3) are registered in historical records for the time-span corresponding to the maximum at 20 m depth (1971 +2/–4 years). For the 44 m maximum, three large volcanic eruptions are recorded in the years 1924 (Raikoke, Kurile Islands, Russia; VEI = 4), 1918 (Katla, Iceland; VEI = 4) and 1912 (Katmai, Alaska, USA; VEI = 6) (Simkin and Siebert, 1994). Dating by counting Na^+ cycles leads to an age of 1924 +2/–4 years for this horizon, and the eruption of Raikoke in 1924 therefore best fits with this event. However, this result contradicts the study of Schütt and others (2003), who assigned the 44 m maximum in the electrical conductivity record to the eruption of Katmai in 1912. This assumption was based on the strength of the event (VEI = 6). Furthermore, the construction of a continuous layer thickness curve for the whole deep ice core by means of the $\delta^{18}O$ and conductivity signal supports Katmai as the source, where further potential volcanoes (e.g. Laki, 1783; VEI = 4; Simkin and Siebert, 1994) have been considered. Note however, that sulphur emission is not a primary parameter in the definition of the VEI (Simkin and Siebert, 1994). Thus, highly explosive eruptions do not necessarily imply high sulphur output and vice versa.

At this stage it is not possible to decide unambiguously which volcanic eruption causes the high conductivity or whether it is a result of melting/refreezing processes. Therefore, microscopic analysis of microparticles to identify the potential presence of volcanic glasses might be helpful. The chemical analysis should be continued to identify additional volcanoes as external reference horizons and to achieve a continuous depth-to-age relation for the whole core. A synthesis of these results with the approach from Schütt and others (2003) may lead to a consistent depth scale for this ice core.

3.5. Long-term variations

As shown above, the seasonal information in the ion signal of the ice from Akademii Nauk reflects primarily seasonal melting/refreezing processes rather than seasonal variations in atmospheric aerosol concentrations. Owing to the large fraction of refrozen ice per annual layer, it is not even certain that all the ions deposited in a specific year are conserved in the respective layer. They may elute to layers below. However, averages of ion concentration on longer timescales where melting/refreezing processes are in balance (i.e. within a few years) should be representative of changes in the atmospheric load, at least for conservative species like sulphate and sodium, where no post-depositional losses via the gas phase occur. Accordingly, we calculated water-weighted, 5 year running averages for non-sea-salt sulphate, nitrate and sodium concentrations in snow over the time-span 1906–99. As clearly illustrated by the grey dots in Figure 6a and b, the anthropogenically influenced species, SO_4^{2-} and NO_3^-, are subject to a substantial increase starting in the 1960s and also to short-term events caused by the specific events discussed above. Because those horizons may be attributed to singular volcanic events, we removed the affected samples (about five samples per horizon) from the dataset and calculated corrected 5 year averages (open circles in Fig. 6). In the following the corrected long-term variations are discussed.

3.5.1. Sulphate

As depicted in Figure 6a, background nssSO_4^{2-} concentrations decreased by about 100 ng g^{-1} at the beginning of the 20th century, then gradually increased by about 100 ng g^{-1} in the following 30 years, until an intermittent decline around 1940. In the mid-1960s, however, sulphate concentrations show an extraordinary rise to background concentrations higher than 400 ng g^{-1}, unprecedented in the decades before. For comparison, we calculated running averages for Na^+, which as a sea-salt tracer is of natural origin only (see section 3.2). The latter shows no long-term increase after 1960 (Fig. 6c). This implies that the trends in sulphate (and nitrate; see below) do not reflect an increase of the load related to melting/refreezing processes as is the case for the discrete events, but can be attributed to a long-term anthropogenic influence on the atmospheric sulphur load. Note also that after maximum concentrations were reached in the mid-1970s, nssSO_4^{2-} concentrations declined steadily

to values below 200 ng g^{-1} in the 1990s, reflecting a substantial reduction in the anthropogenic sulphur load during recent decades.

Owing to the significant variation in background concentrations at the beginning of the last century, it is difficult to define a representative early-industrial to pre-industrial level. Taking into account that around 1910 we find a significant number of smaller sulphate peaks in the record, which might also be related to less pronounced volcanic depositions expected for this time interval, we estimate average early-industrial sulphate concentrations in Figure 6a to be 100–120 ng g^{-1}. Thus, industrial emissions after 1965 lead to a four-fold increase in sulphate concentrations in only a few years, implying dramatic ecological consequences for the High Arctic. As a matter of fact, in the raw data this rise takes place within only 1–2 years and indicates rapid increases in additional emission sources relevant for Severnaya Zemlya.

Comparison of the Severnaya Zemlya with other Northern Hemisphere sulphate ice-core records shows no such dramatic and sudden rise in Greenland records (Mayewski and others, 1990; Legrand and Mayewski, 1997; Fischer and others, 1998b) or in records from Svalbard (e.g. Goto-Azuma, 1995; Simões and Zagarodnov, 2001) or Penny Ice Cap (Grumet and others, 1998; Goto-Azuma and Koerner, 2001). This points to proximal sources being more important for the Akademii Nauk ice core. The records from Svalbard also indicate an increase in the second half of the 20th century. However, sulphate concentrations in these cores increase by a factor of only two in the course of the 20th century, and for Snøfjellafonna (Goto-Azuma and others, 1995) the increase is more gradual and starts at around 1950. A sudden rise in SO_4^{2-} concentrations at the end of the 1960s in that record is counterbalanced by a pronounced minimum in layers above, pointing to a melting/refreezing feature and not to a comparable change in the atmospheric load. The Greenland records (Mayewski and others, 1990; Fischer and others, 1998b) reveal a more gradual increase in sulphate concentration over the last century than any of the lower-altitude Arctic ice cores. This gradual rise has been attributed to the increase of total Eurasian sulphur dioxide emissions (Mylona, 1996) in the 20th century (Fischer and others, 1998b). The sudden rise at Severnaya Zemlya is not in line with a gradual increase in total Eurasian sources, as clearly illustrated in Figure 6a (squares). While Greenland is remote from all industrial sources and, with its high altitude, is more representative of tropospheric background conditions, the proximity of Akademii Nauk to the Norilsk mining complex in Siberia and to mining locations on the Kola peninsula, and its much lower altitude, points to more regional emission sources. Thus, the sudden rise in sulphate concentrations around 1966 +2/–4 years may point to an increase in emission rates from these sites. Indeed, a major shift from the use of low-sulphur nickel ore of local origin to ore from Norilsk with extremely high sulphur content is reported for the Kola region during the mid-1960s (personal communication from A. Ryaboshapko). No information on the temporal development of sulphur emission is available for the Norilsk region for that time. Nowadays, Norilsk is the most important point source of sulphur in the former USSR, with annual emissions of 1.2 and 1.1 $\times 10^9$ kg S a^{-1} in 1985 and 1990, respectively (Ryaboshapko and others, 1996). Model results on sulphur dioxide and sulphate transport in the Arctic by Christensen (1997) support an important contribution to inner Arctic sulphur levels by the nickel- and copper-producing industries on the Kola peninsula and in Norilsk. Also, back trajectory studies by Vinogradova and Egorov (1996) clearly show the dominant influence of air masses originating over central Siberia for the aerosol transport onto Severnaya Zemlya. Furthermore, elemental tracer studies on the aerosol composition at the coastal sites Point Barrow, Alaska (Rahn and Loewenthal, 1986), and Svalbard (Pacyna, 1991) reveal a dominant influence of anthropogenic emission from sources located in the central part of the former USSR during the early 1980s, not only for the Eurasian but also for the North American sector of the Arctic. In summary, we conclude that a primary influence of regional Siberian industrial emissions on the sulphate levels in Severnaya Zemlya is most likely.

Assuming that the hypothesis of regional industrial sources in Siberia being the dominant influence on sulphate deposition on Severnaya Zemlya is correct, the measured reduction in sulphate snow concentrations over recent decades would also imply a decrease of emissions from these sites, possibly related to an economic decline of the companies in Norilsk and the Kola peninsula.

3.5.2. Nitrate

In Figure 6b the nitrate background concentrations show a very similar temporal evolution to the sulphate levels. A systematic decrease of NO_3^- from about 70 ng g^{-1} in 1910 to about 50 ng g^{-1} in 1940 is followed by 20 ng g^{-1} higher concentrations around 1950. The major increase, however, is from a local minimum of 55 ng g^{-1} in the early 1960s to >160 ng g^{-1} in the 1970s. Thus, nitrate concentrations have risen by a factor of three since early-industrial levels at the start of the last century. As was the case for the sulphate raw data, major parts of this increase occurred in a 1–2 year step at 1966 +2/–4 years.

Again, no such step increase in NO_3^- concentrations can be found in the Greenland records (Mayewski and others, 1990; Legrand and Mayewski, 1997; Fischer and others, 1998b); however, it is indicated by records from smaller ice caps in Svalbard and the Canadian Arctic (Goto-Azuma, 2001; Kekonen and others, 2002). The ice core from Lomonosovfonna, Svalbard, (Kekonen and others, 2002) shows an increase to about 200 ng g^{-1} both in the late 1950s and during the period 1970–85. The first of these increases is not clearly found on Severnaya Zemlya. The record from Snøfjellafonna shows an outstanding maximum in nitrate concentrations around 1968, at least partly related to melt processes (see above). Total European NO_x emissions (Hov and others, 1987) as depicted in Figure 6b rose gradually starting in the 1940s and can therefore not explain the step increase in nitrate concentrations on Severnaya Zemlya. Even more striking is the nitrate decline by 70–100 ng g^{-1} synchronous with the decrease of sulphate concentrations in the last two decades. Such a significant nitrate decrease is not found in the Greenland records. Accordingly, this result rules out a comparable anthropogenic source mix for both regions and strongly points to regional NO_x emissions by industrial combustion processes occurring in the Siberian Arctic, leading to drastic changes in nitrate concentrations on Severnaya Zemlya.

4. CONCLUSIONS AND OUTLOOK

This study has shown that even if the chemical signal in the ice core from Akademii Nauk is disturbed due to annually

occurring melt processes, information about the aerosol composition of the past atmosphere can still be deduced. Long-term variations in anthropogenic sulphate and nitrate precursors could be determined from the ice-core records, where the sulphate trend can probably be ascribed to the nickel- and copper-producing industries at Norilsk or the Kola peninsula, as the principal inner Arctic sources.

In contrast, the cyclic behaviour observed in the ion records cannot be assigned to the seasonal variation in atmospheric aerosol concentrations. Rather, these variations reflect a melting/refreezing signal from which, however, a depth-to-age relation can be derived. Thus, it was possible to achieve continuous dating of the first 53 m of the ice core by counting cycles in the Na^+ record. Using this approach, the depth interval investigated in this study reflects a time-span of around 100 years, and a mean annual net mass balance through the 20th century of 0.46 m w.e. a^{-1} was deduced for Severnaya Zemlya.

Peaks in electrical conductivity in ice cores drilled in the percolation snow zone are not necessarily linked to volcanic events. An exceptionally high maximum at around 26 m depth could be attributed to the eruption of Bezymianny in 1956, but the ionic composition of two peaks at approximately 20 and 44 m depth did not give unambiguous evidence for a volcanic input. Thus, it has to be expected that only a few reference horizons will be available to date a deep ice core.

To improve insight into the melt processes, more detailed investigations of the core stratigraphy may be helpful. With such information it could also be possible to estimate the time-scale for which an atmospheric signal can be deduced from the chemical composition of the ice, i.e. the number of annual layers which are penetrated by the meltwater of one season.

ACKNOWLEDGEMENTS

We thank B. Twarloh for help with the chemical analysis of the ice samples. We thank R. Schütt for useful comments on the manuscript. This project is funded by the German Ministry of Education and Research (BMBF research project 03PL 027A). It is a joint venture of the Alfred Wegener Institute for Polar and Marine Research, Germany, and the Arctic and Antarctic Research Institute and the Mining Institute, both in St Petersburg, Russia.

REFERENCES

Alexandrov, E.I., V.F. Radinov and P.N. Svyashchennikov. 2000. Climate regime and its changes in the region of the Barents and Kara seas. *In Transport and fate of contaminents in the northern seas. Sea ice project package*. Arctic and Antarctic Research Institute, Chapter 3. (AARI final report.)

Arkhipov, S.M. 1999. Data bank "Deep drilling of glaciers: Soviet and Russian projects in Arctic, 1975–1990" [Isotope glaciology in the USSR and Russia.]. *Mater. Glyatsiol. Issled./Data Glaciol. Stud.,* **87**, 229–231. [In English with Russian summary.]

Beer, J. *and 15 others*. 1991. Seasonal variations in the concentrations of ^{10}Be, Cl^-, NO_3^-, SO_4^{2-}, H_2O_2, ^{210}Pb, ^3H mineral dust and $\delta^{18}O$ in Greenland snow. *Atmos. Environ., Ser. A,* **25**(5–6), 899–904.

Benson, C.S. 1961. Stratigraphic studies in the snow and firn of the Greenland ice sheet. *Folia Geogr. Dan.,* **9**, 13–37.

Christensen, J.H. 1997. The Danish Eulerian Hemispheric Model: a three-dimensioral air pollution model used for the Arctic. *Atmos. Environ.,* **31**(24), 4169–4191.

Davidson, C.I. *and. others*. 1993. Chemical constituents in the air and snow at Dye 3, Greenland: 1. Seasonal variations. *Atmos. Environ., Ser. A,* **27**(17–18), 2709–2722.

Davies, T.D., C.E. Vincent and P. Brimblecombe. 1982. Preferential elution of strong acids from a Norwegian ice cap. *Nature,* **300**(5888), 161–163.

Davis, R.E., C.E. Petersen and R.C. Bales. 1995. Ion flux through a shallow snowpack: effects of initial conditions and melt sequences. *International Association of Hydrological Sciences Publication* 228 (Symposium at Boulder 1995 – *Biogeochemistry of Seasonally Snow-Covered Catchments*), 115–126.

Fischer, H., D. Wagenbach and J. Kipfstuhl. 1998a. Sulfate and nitrate firn concentrations on the Greenland ice sheet. 1. Large-scale geographical deposition changes. *J. Geophys. Res.,* **103**(D17), 21,927–21,934.

Fischer, H., D. Wagenbach and J. Kipfstuhl. 1998b. Sulfate and nitrate firn concentrations on the Greenland ice sheet. 2. Temporal anthropogenic deposition changes. *J. Geophys. Res.,* **103**(D17), 21,935–21,942.

Fritzsche, D. *and 6 others*. 2002. A new deep ice core from Akademii Nauk ice cap, Severnaya Zemlya, Eurasian Arctic: first results. *Ann. Glaciol.,* **35**, 25–28.

Goto-Azuma, K. and R.M. Koerner. 2001. Ice core studies of anthropogenic sulfate and nitrate trends in the Arctic. *J. Geophys. Res.,* **106**(D5), 4959–4969.

Goto-Azuma, K., H. Enomoto, S. Takahashi, S. Kobayashi, T. Kameda and O. Watanabe. 1993. Leaching of ions from the surface of glaciers in western Svalbard. *Bull. Glacier Res.,* **11**, 39–50.

Goto-Azuma, K. *and 6 others*. 1995. An ice-core chemistry record from Snöfjellafonna, northwestern Spitsbergen. *Ann. Glaciol.,* **21**, 213–218.

Grumet, N.S., C.P. Wake, G.A. Zielinski, D. Fisher, R. Koerner and J.D. Jacobs. 1998. Preservation of glaciochemical time-series in snow and ice from the Penny Ice Cap, Baffin Island. *Geophys. Res. Lett.,* **25**(3), 357–360.

Herron, M.M. 1982. Impurity sources of F^-, Cl^-, NO_3^- and SO_4^{2-} in Greenland and Antarctic precipitation. *J. Geophys. Res.,* **87**(C4), 3052–3060.

Hov, Ø. *and 8 others*. 1987. *Evaluation of atmospheric processes leading to acid deposition in Europe*. Brussels, Commission of the European Communities. (Air Pollution Research Report 10.)

Johannessen, M. and A. Henriksen. 1978. Chemistry of snow meltwater: changes in concentration during melting. *Water Resour. Res.,* **14**(4), 615–619.

Kahl, J.D.W., D.A. Martinez, H. Kuhns, C.I. Davidson, J.-L. Jaffrezo and J.M. Harris. 1997. Air mass trajectories to Summit, Greenland: a 44-year climatology and some episodic events. *J. Geophys. Res.,* **102**(C12), 26,861–26,875.

Kekonen, T., J.C. Moore, R. Mulvaney, E. Isaksson, V. Pohjola and R.S.W. van de Wal. 2002. An 800 year record of nitrate from the Lomonosovfonna ice core, Svalbard. *Ann. Glaciol.,* **35**, 261–265.

Kotlyakov, V.M., S.M. Arkhipov, K.A. Henderson and O.V. Nagornov. 2004. Deep drilling of glaciers in Eurasian Arctic as a source of paleoclimate records. *Quat. Sci. Rev.,* **23**(11–13), 1371–1390.

Kuhn, M. 2000. Severnaja automatic weather station data (Severnaja Zemlja). In *The response of Arctic ice mass to climate change (ICEMASS)*. Third Year Report (January–December 2000). European Commission, Framework IV, Environment and Climate Research Programme (DG XII), contract ENV4-CT97–0490. Oslo, University of Oslo, 7–8–7–14.

Legrand, M. and P. Mayewski. 1997. Glaciochemistry of polar ice cores: a review. *Rev. Geophys.,* **35**(3), 219–243.

Mayewski, P.A., W.B. Lyons, M.J. Spencer, M.S. Twickler, C.F. Buck and S. Whitlow. 1990. An ice core record of atmospheric response to anthropogenic sulphate and nitrate. *Nature,* **346**(6284), 554–556.

Mulvaney, R., E.W. Wolff and K. Oates. 1988. Sulphuric acid at grain boundaries in Antarctic ice. *Nature,* **331**(6153), 247–249.

Mylona, S. 1996. Sulphur dioxide emissions in Europe 1880–1991 and their effect on sulphur concentrations and deposition. *Tellus,* **48**(5), 662–689.

Pacyna, J.M. 1991. Chemical tracers of the origin of Arctic air pollution. *In* Sturges, W.T., *ed. Pollution of the Arctic atmosphere*. Essex, Elsevier Science Publishers Ltd, 97–122.

Pinglot, J.F. *and 13 others*. 2003. Ice cores from Arctic sub-polar glaciers: chronology and post-depositional processes deduced from radioactivity measurements. *J. Glaciol.,* **49**(164), 149–158.

Rahn, K.A. and D.H. Loewenthal. 1986. Who's polluting the Arctic? Why is it important to know? An American perspective. *In* Stonehouse, B., *ed. Arctic air pollution*. Cambridge, Cambridge University Press, 85–95.

Rahn, K.A., R.D. Borys and G.E. Shaw. 1977. Particulate air pollution in the Arctic: large-scale occurrence and meteorological controls. *In* Roddy, A.G. and T.C. O'Connor, *eds. Ninth International Conference on Atmospheric Aerosols and Nuclei, Galway, Ireland, 21–27 September 1977. Proceedings*. Galway, Galway University Press, 223–227.

Ryaboshapko, A., P.A. Brukhanov, S.A. Gromov, Y.V. Proshina and O.G. Afinogenova. 1996. *Anthropogenic emissions of oxidized sulfur and nitrogen into the atmosphere of the former Soviet Union in 1985 and 1990.* Stockholm, Department of Meteorology, Stockholm University and International Meteorological Institute in Stockholm. (Report CM-89.)

Schütt, R., D. Fritzsche, H. Meyer, H. Miller, F. Wilhelms and H. Hubberten. 2003. Auferstanden auf Ruinen – ein sibirisches Gletserleben im Holozän. *In 6. Deutsche Klimatagung Klimavariabilität, Potsdam, Germany, 22–25 September 2003. Terra Nostra, Schriften der Alfred Wegener Stiftung,* **6**, 389–393.

Shaw, G.E. 1995. The Arctic haze phenomenon. *Bull. Am. Meteorol. Soc.,* **76**(12), 2403–2413.

Simkin, T. and L. Siebert. 1994. *Volcanoes of the world. Second edition.* Tucson, AZ, Geoscience Press.

Simões, J.C. and V.S. Zagorodnov. 2001. The record of anthropogenic pollution in snow and ice in Svalbard, Norway. *Atmos. Environ.,* **35**(2), 403–413.

Steffensen, J.P. 1988. Analysis of the seasonal variation in dust, Cl^-, NO_3^- and SO_4^{2-} in two central Greenland firn cores. *Ann. Glaciol.,* **10**, 171–177.

Vaikmyae, R.A. and Y.-M.K. Punning. 1982. Izotopno-geokhimicheskiye issledovaniya na lednikovom kupole Vavilova, Severnaya Zemlya [Isotopic and geochemical studies on the Vavilov ice dome in Severnaya Zemlya]. *Mater. Glyatsiol. Issled.,* **44**, 145–149. [In Russian with English summary.]

Vinogradova, A.A. and V.A. Egorov. 1996. Long-range pollutant transport into the Russian Arctic. *Izvestiia Akademii Nauk SSSR, Fizika Atmosfery i Okeana [Atmospheric and Oceanic Physics],* **32**(6), 796–802.

Wilhelms, F. 2000. Messung dielektrischer Eigenschaften polarer Eiskerne. *Ber. Polarforsch./Rep. Pol. Res.,* **367**, 1–171.

Wilhelms, F., D. Fritzsche, J. Kipfstuhl, H. Miller, M. Schwager and T. Thorsteinsson. 1997. Continuous physical properties from the NGRIP ice core. *Eos,* **78**(46), Fall Meeting Supplement, F8.

Wilhelms, F., J. Kipfstuhl, H. Miller, K. Heinloth and J. Firestone. 1998. Precise dielectric profiling of ice cores: a new device with improved guarding and its theory. *J. Glaciol.,* **44**(146), 171–174.

Zagorodnov, V.S., O.L. Klementyev, N.N. Nikiforov, V.I. Nikolaëv, L.M. Savatyugin and V.A. Sasunkevich. 1990. Gidroterminicheskiy rezhim i l'doobrazovaniye v tsentral'noy chasti lednika Akademii Nauk na Severnoy Zemle [Hydrothermal regime and ice formation in the central part of the Akademiya Nauk glacier, Severnaya Zemlya]. *Mater. Glyatsiol. Issled.,* **70**, 36–43. [In Russian with English summary.]

MS received 30 October 2003 and accepted in revised form 28 October 2004